KeV Astrophysics With GeV Beams; Blazing a New Trail on the Summitt of Nuclear Astrophysics *

Moshe Gai

Laboratory for Nuclear Science, Dept. of Physics, U3046,
University of Connecticut, 2152 Hillside Rd., Storrs, CT 06269-3046, USA
(gai@uconn.edu, http://www.phys.uconn.edu)

February 1, 2008

Abstract

GeV beams of light ions and electrons are used for creating a high flux of real and virtual photons, with which some problems in Nuclear Astrophysics are studied. GeV ^8B beams are used to study the Coulomb dissociation of ^8B and thus the $^7Be(p,\gamma)^8B$ reaction. This reaction is one of the major source of uncertainties in estimating the ^8B solar neutrino flux and a critical input for calculating the ^8B Solar neutrino flux. The Coulomb dissociation of ^8B appears to provide a viable method for measuring the $^7Be(p,\gamma)^8B$ reaction rate, with a weighted average of the RIKEN1, RIKEN2, GSI1 and MSU published results of $S_{17}(0) = 18.9 \pm 1.0$ eV-b. This result however does not include a theoretical error estimated to be $\pm 10\%$. GeV electron beams on the other hand, are used to create a high flux of real and virtual photons at TUNL-HIGS and MIT-Bates, respectively, and we discuss two new proposals to study the $^{12}C(\alpha,\gamma)^{16}O$ reaction with real and virtual photons. The $^{12}C(\alpha,\gamma)^{16}O$ reaction is essential for understanding Type II and Type Ia supernova. It is concluded that virtual and real photons produced by GeV light ions and electron beams are useful for studying some problems in Nuclear Astrophysics.

1

1 Introduction: The $^7Be(p,\gamma)^8B$ Reaction at Low Energies

The solar neutrino problem [1, 2] may allow for new break through in neutrino physics and the standard model of particle physics. The precise knowledge of the astrophysical S_{17}-factor $[= \sigma_{17} \times E \times exp(2\pi\eta)$ where η is the Sommerfeld parameter $= Z_1 Z_2 \frac{\alpha}{\beta})$, is crucial for interpreting terrestrial measurements of the solar neutrino flux [3]. This is particularly true for the interpretation of results from the Homestake, Kamiokande, SuperKamiokande and SNO experiments [2] which measured high energy solar neutrinos mainly or solely from ^{8}B decay. In Fig. 1 we show the world data including our new GSI measurement of S_{17} [4]. It is clear from this figure that if we are to quote $S_{17}(0)$ with an accuracy of $\pm5\%$, many more experiments using different methods are required.
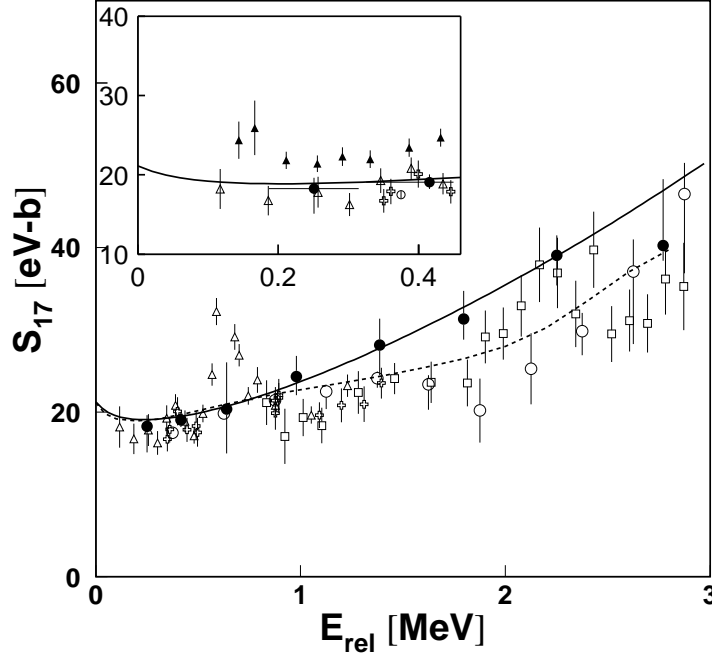

Fig. 1: World data on S_{17} as reported by our GSI collabortion [4].

2 The Coulomb Dissociation of ^8B and the $^7Be(p,\gamma)^8B$ Reaction at Low Energies

The Coulomb Dissociation (CD) [5, 6] is a Primakoff [7] process that could be viewed in first order as the time reverse of the radiative capture reaction. The large relative velocities of light ion beams create a large flux of virtual photons and instead of studying for example the fusion of a proton plus a nucleus (A-1), one studies the disintegration of the final nucleus (A) in the Coulomb field, to a proton plus the (A-1) nucleus. The reaction is made possible by the absorption of a virtual photon from the field of a high Z nucleus such as ^{208}Pb. In this case since π/k^2 for a photon is approximately 100-1000 times larger than that of a particle beam, the small cross section is enhanced. The large virtual photon flux (typically 100-1000 photons per collision) also gives rise to enhancement of the cross section. Our understanding of the Coulomb dissociation process [5, 6] allows us to extract the inverse nuclear process even when it is very small. However in Coulomb dissociation since αZ approaches unity (unlike the case in electron scattering), higher order Coulomb effects (Coulomb post acceleration) may be non-negligible and they need to be understood [8, 9]. The success of CD experiments [10] is in fact contingent on understanding such effects and designing the kinematical conditions so as to minimize such effects.

Hence the Coulomb dissociation process has to be measured with great care with kinematical conditions carefully adjusted so as to minimize nuclear interactions (i.e. distance of closest approach considerably larger then 20 fm, or very small forward angles scattering), and measurements must be carried out at high enough energies (many tens of MeV/u) so as to maximize the virtual photon flux.

2.1 The GSI Results at 254 A MeV

An experiment to measure the Coulomb dissociation of ^{8}B at a higher energy of 254 A MeV was performed at GSI [4]. The present experimental conditions have several advantages: (i) forward focusing allows us to use the magnetic spectrometer KaoS [11] at GSI for a kinematically complete measurement with high detection efficiency over a wider range of the p-^{7}Be relative energy; (ii) because of the smaller influence of straggling on the experimental resolution at the higher energy, a thicker target can be used for compensating

3

the weaker beam intensity, (iii) effects that obscure the contribution of E1 multipolarity to the Coulomb dissociation like E2 admixtures and higher-order contributions are reduced [8, 9]. The contribution of M1 multipolarity is expected to be enhanced at the higher energy, but this allows to observe the M1 resonance peak and determine its γ width.

A ^{8}B beam was produced by fragmentation of a 350 A MeV ^{12}C beam from the SIS synchrotron at GSI that impinged on a beryllium target with a thickness of 8.01 g/cm^2. The beam was isotopically separated by the fragment separator (FRS) [12] by using an aluminum degrader with a thickness of 1.46 g/cm^2 with a wedge angle of 3 mrad. The beam was transported to the standard target-position of the spectrometer KaoS [11]. The average beam energy of ^{8}B in front of the breakup target was 254.5 A MeV, a typical ^{8}B intensity was 10^4 /spill (7s/spill). Beam-particle identification was achieved event by event with the TOF-ΔE method by using a beam-line plastic scintillator with a thickness of 5 mm placed 68 m upstream from the target and a large-area scintillator wall discussed later placed close to the focal plane of KaoS. About 20 % of the beam particles were ^{7}Be, which could however unambiguously be discriminated from breakup ^{7}Be particles by their time of flight.

An enriched ^{208}Pb target with a thickness of 199.7 ($\pm$ 0.2) mg/cm^2 was placed at the entrance of KaoS. The average energy at the center of the target amounted to 254.0 A MeV. The reaction products, ^{7}Be and proton, were analyzed by the spectrometer which has a large momentum acceptance of $\Delta p/p \approx 50$ % and an angular acceptance of 140 and 280 mrad in horizontal and vertical directions, respectively. For scattering-angle measurement or track reconstruction of the two reaction products, two pairs of silicon micro-strip detectors were installed at about 14 and 31 cm downstream from the target, respectively, measuring either x- or y-position of the products before entering the KaoS magnets. Each strip detector had a thickness of 300 μm, an active area of 56×56 mm^2, and a strip pitch of 0.1 mm.

The measured complete kinematics of the breakup products allowed us to reconstruct the p-^{7}Be relative energy and the scattering angle θ_8 of the center-of-mass of proton and ^{7}Be (excited ^{8}B) with respect to the incoming beam from the individual momenta and angles of the breakup products.

To evaluate the response of the detector system, Monte-Carlo simulations were performed using the code GEANT[13]. The simulations took into account the measured ^{8}B beam spread in energy, angle, and position at the target, as well as the influence of angular and energy straggling and energy

loss in the layers of matter. Losses of the products due to limited detector sizes were also accounted for. Further corrections in the simulation are due to the feeding of the excited state at 429 keV in ^{7}Be. We used the result by Kikuchi *et al.* [14] who measured the γ-decay in coincidence with Coulomb dissociation of ^{8}B at 51.9 A MeV.

The Monte Carlo simulations yielded relative-energy resolutions from the energy and angular resolutions of the detection system to be 0.11 and 0.22 MeV (1σ) at $E_{\rm rel} = 0.6$ and 1.8 MeV, respectively. The total efficiency calculated by the simulation was found to be larger than 50% at $E_{\rm rel} = 0 - 2.5$ MeV. due to the large acceptance of KaoS. The experimental angular distributions are well reproduced by the simulation using only E1 multipolarity, in line with the results of Kikuchi *et al.* [14] and Gai and Bertulani [10].

To study our sensitivity to a possible E2 contribution, we have added the simulated E2 angular distribution from the E2 Coulomb dissociation cross section calculated by Bertulani and Gai [15]. Note that nuclear breakup effects are also included in the calculation. By fitting the experimental angular distributions to the simulated ones, we obtained 3σ upper limits of the ratio of the E2- to E1-transition amplitude of the ^{7}Be(p,γ)^{8}B reaction, $S_{\rm E2}/S_{\rm E1}$ of 0.06×10^{-4}, 0.3×10^{-4} and 0.6×10^{-4} for $E_{\rm rel} = 0.3 - 0.5$, $0.5 - 0.7$ and $1.0 - 1.2$ MeV, respectively. These numbers agree well with the results of Kikuchi *et al.* [14], and suggest that the results of the model dependent analysis of Davids *et al.* [17] needs to be checked. The MSU collaboration recently also published values for $S_{17}(0)$ [18] which are in agreement with the arlier results of the RIKEN II experiment [19].

2.2   Conclusion: The Coulomb Dissociation Method

In conclusion we demonstrated that the Coulomb dissociation (when used with "sechel") provides a viable alternative method for measuring small cross section of interest for nuclear-astrophysics. First results on the CD of ^8B are consistent with the lower measured values of the cross section and weighted average of all thus far data is: $S_{17}(0) = 18.9 \pm 1.0 \ eV - b$, see Table 1. The accuracy of the extracted S-factors are now limited by our very understanding of the Coulomb dissociation process, believed to be approx. $\pm 10\%$. The value of the E2 S-factor as extracted from both the RIKEN and GSI experiments are consistent and shown to be very small, S_{E2}/S_{E1} of the order of 10^{-5} or smaller, see Table 1. The adopted value of S_{17} from the

CD experiments, shown in Table I is in good agreement with recent direct measuremenst [20, 21].

Table 1: Measured S-factors in Coulomb dissociation experiments.

Experiment	$S_{17}(0)$ eV-b	$S_{E2}/S_{E1}(0.6$ MeV$)$
RIKEN1	16.9 ± 3.2	$< 7 \times 10^{-4}$
RIKEN2	18.9 ± 1.8	$< 4 \times 10^{-5}$
GSI1	$20.6 \ + 1.2 \ - 1.0$	$< 3 \times 10^{-5}$
GSI2	?	?
MSU	$17.8 \ + 1.4 \ - 1.2$	$4.7 \ + 2.0 \ - 1.3 \times 10^{-4}$
ADOPTED	18.9 ± 1.0	$< 3 \times 10^{-5}$

3 Introduction: Oxygen Formation in Helium Burning and The $^{12}C(\alpha, \gamma)^{16}O$ Reaction

The outcome of helium burning is the formation of the two elements, carbon and oxygen [22, 23, 24]. The ratio of carbon to oxygen at the end of helium burning is crucial for understanding the fate of a Type II supernovae and the nucleosynthesis of heavy elements. While an oxygen rich star is predicted to end up as a black hole, a carbon rich star leads to a neutron star [23]. At the same time helium burning is also very important for understanding Type Ia supernovae (SNIa) now used as a standard candle for cosmological distances [25]. All thus far luminosity calibration curves and the stretching parameter are used as empirical observation without fundamental understanding between the time characteristics of the light curve and the luminosity of a Type Ia supernova. Since the first burning stage in helium burning, the triple alpha-particle capture reaction ($^{8}Be(\alpha, \gamma)^{12}C$), is well understood [22], one must extract the p-wave [$S_{E1}(300)$] and d-wave [$S_{E2}(300)$] cross section

of the $^{12}C(\alpha,\gamma)^{16}O$ reaction at the Gamow peak (300 keV) with high accuracy of approximately 10% or better to completely understand stellar helium burning. An independent R-matrix analysis [26] of all available data can not rule out a small S-factor solution (10-20 keV-b). It is thus doubtful that one can indeed rule out a small E1 S-factor solution based on current data. The confusion in this field mandates a direct measurement of the cross section of the $^{12}C(\alpha,\gamma)^{16}O$ reaction at low energies at energies even .

4   The Proposed $^{16}O(\gamma,\alpha)^{12}C$ and $^{16}O(e,e'\alpha)^{12}C$ Experiments

For determination of the cross section of the $^{12}C(\alpha,\gamma)^{16}O$ at very low energies, as low as $E_{cm} = 700$ KeV considerably lower than measured till now [27], it is advantageous to have an experimental setup with larger (amplified) cross section, high luminosity and low background. It turns out that the use of the inverse process, the $^{16}O(\gamma,\alpha)^{12}C$ reaction may indeed satisfy all three conditions. The cross section of $^{16}O(\gamma,\alpha)^{12}C$ reaction (with polarized photons) at the kinematical region of interest (photons approx 8-8.5 MeV) is larger by a factor of approximately 100 than the cross section of the direct $^{12}C(\alpha,\gamma)^{16}O$ reaction. Note that the polarization yields an extra factor of two in the enhancement. Thus for the lowest data point measured at 0.9 MeV with the direct cross secion of approx. 60 pb, the photodissociation cross section is 6 nb. It is evident that with similar luminosities and lower background, see below, the photodissociation cross section can be measured to yet lower center of mass energies, as low as 0.7 MeV, where the direct $^{12}C(\alpha,\gamma)^{16}O$ crosssection is of the order of 1 pb. However, we cannot observe cascade gamma decay, which are considered to be small at low energies.

The High Intensity Gamma Source (HIGS) [28], shown in Fig. 2, has already achieved many milestones and is rapidly approaching its design goal of 2-200 MeV gammas, with 9 MeV gammas at a resolution of 0.1% and intensity of order 10^9 /sec. Current intensities are of the order of 10^6 /sec and resolution of 0.8The backscattered photons of the HIGS facility are collimated and will enter the target/detector TPC setup as we propose below. With a Q value of -7.162, our experiment will utilize gammas of energies ranging from 8 to 10 MeV. Note that the emitted photons are linearly polarized [29] and the emitted particles are primarily in a horizontal plane with a

$sin^2\phi$ azimuthal angular dependence [31]. This simplifies the tracking of particles in this experiment. The pulsed photon beam provides a trigger for the image intensified CCD camera, and the time projection information from the chamber yields the azimuthal angle of the event of interest. Background events will be discriminated with time of flight techniques, and flushing of the CCD between two events. To reduce noise, the CCD will be cooled. We note that similar research program with high intensity photon beams and a TPC already exists at the Tokyo Institute of Technology [30]. An $^{16}O(e, e'\alpha)^{12}C$ is proposed at the MIT-Bates accelerator [32]. This meausrement with virtual photons is sensitive mostly to d-wave astrophysical cross section factor.
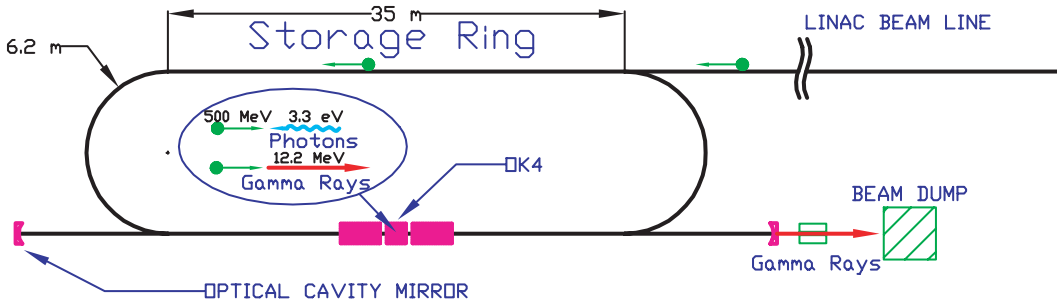

Fig. 2: Schematic diagram of the HIGS facility [28] for the production of intense MeV gamma beams.

4.1   Proposed Time Projection Chamber (TPC)

We intend to construct an Optical Readout Time Projection Chamber (TPC), similar to the TPC constructed in the Physikalisch Technische Bundesanstalt, (PTB) in Braunschweig, Germany and the Weizmann Institute, Rehovot, Israel [33], for the detection of alphas and carbon, the byproduct of the photodissociation of ^{16}O. Since the range of available alphas is approximately 8 cm (at 100 mbars) the TPC will be 30 cm wide and up to one meter long for later phases of our studies. We intend first to construct a 30 cm long TPC prototype and place it on the HIGS beam line at TUNL/Duke. The TPC that we intend to construct will be largely insensitive to single Compton electrons, but will allow us to track both alphas and carbons emitted almost back to back in time correlation. The very different range of alphas and carbons (approx. a factor of 4), and differences in the lateral ionization density, will aid us in particle identification. Such a TPC detector would also allow us to

8

measure angular distributions with respect to the polarization vector of the photon thus seperating the E1 and E2 components of the $^{12}C(\alpha, \gamma)^{16}O$ reaction. The excellent energy resolution of the TPC (approx. 2%) allows us to exclude events from the photodissociation of nuclei other than ^{16}O, including isotopes of carbon, oxygen and fluorine, which may also be present in the gas. In Fig. 3, taken from Titt *et al.* [33], we show a schematic diagram of the Optical Readout TPC we proposed to construct. A photon beam enters the TPC through an entrance hole in the drift chamber part of the TPC and mainly produce background e^+e^- pair and a smaller amount of compton electrons, as well as the photodissociation of various nuclei present in the $CO_2 + Ar$ gas mixture, including ^{16}O. As we discuss later the background events are easily rejected.
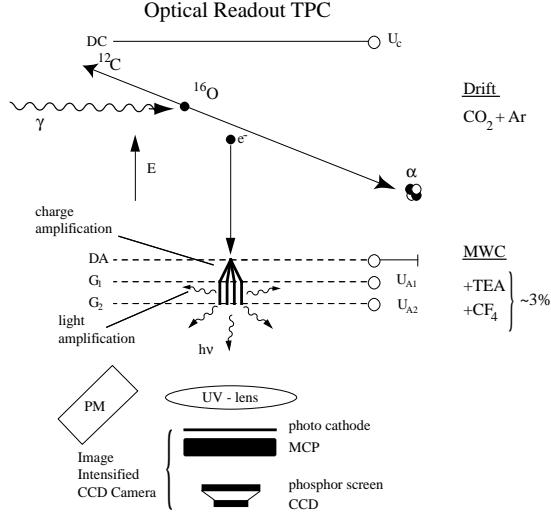

Fig. 3: Schematic diagram of the Optical Readout TPC [33].

The charged particle byproducts of the photodissociation create delta electrons that create secondary electrons that drift in the chamber electric field with a total time of the order of 1 μs for 5 cm. The time projection of the drift electrons allows us to measure the inclination angle (ϕ) of the plane of the byproducts, and the tracks themselves allow for measurement of the scattering angle (θ), both with an accuracy of better than two degrees. The electrons that reach the multi-wire chamber are multiplied (by approx. a factor of 10^7) and interact with a small (3%) admixture of triethylamine (TEA) [33] or CF_4 [34] gas to produce UV or visible photons, respectively. The light detected in the photomultiplier tube, see Fig. 4, triggers the Image Intensifier and CCD camera which takes a picture of the visible tracks. The

9

picture is downloaded to a PC and analyzed for recognition of the two back-to-back alpha-carbon tracks. The background electrons lose approx. 100 keV in the entire TPC and are removed by an appropriate threshold on the Photo Multiplier Tube (PM), and events from the photodissociation of nuclei other than ^{16}O are removed by measuring the total energy (Q-value) of the event.

4.2 Design Goals

The luminosity of a our proposed $^{16}O(\gamma, \alpha)^{12}C$ experiment can be very large. For example, with a 100 cm long target of pure CO_2 at a pressure of 76 torr (100 mbar) and a photon beam of 2×10^9 /sec, we obtain a luminosity of 10^{30} $sec^{-1}cm^{-2}$, or a day long integrated luminosity of 0.1 pb^{-1}. Thus a measurement of the photodissociation of ^{16}O with cross section of 10 pb, with our proposed high efficiency TPC will yield one count per day. Hence it is conceivable that a facility with such luminosity and low background together with the high efficiency TPC will allow us to measure the photodissociation cross section to a few tens of pb and thus as low as several hundreds of fb for the direct $^{12}C(\alpha, \gamma)^{16}O$ reaction, corresponding to energies as low as E_{cm} = 700 keV.

5 Acknowledgement

References

[1] John N. Bahcall, Neutrino Astrophysics, Cambridge University Press, New York, 1989.

[2] J.N. Bahcall, F. Calaprice, A.B. McDonald, and Y. Totsuka; Physics Today**30,#7**(1996)30 and references therein.

[3] E.G. Adelberger *et al.*; Rev. Mod. Phys. **70**(1998)1265.

[4] N. Iwasa *et al.*; Phys. Rev. Lett. **83**(1999)2910

[5] G. Baur, C.A. Bertulani, and H. Rebel; Nucl. Phys. **A458**(1986)188.

[6] C.A. Bertulani and G. Baur; Phys. Rep. **163**(1988)299.

[7] H. Primakoff; Phys. Rev. **81**(1951)899.

[8] C.A. Bertulani; Phys. Rev. **C49**(1994)2688.

[9] S. Typel and G. Baur; Phys. Rev. **C50**(1994)2104.

[10] Moshe Gai, Nucl. Phys. **B(Sup.)38**(1995)77.

[11] P. Senger *et al.*, Nucl. Instr. Meth. A **327**, 393 (1993).

[12] H. Geissel *et al.*, Nucl. Instr. Meth. B **70**, 286 (1992).

[13] Detector description and simulation tool by CERN, Geneva, Switzerland.

[14] T. Kikuchi *et al.*; Phys. Lett. **B391**(1996)261.

[15] Carlos A. Bertulani and Moshe Gai; Nucl. Phys. **A636(1998)227**.

[16] Moshe Gai, and Carlos A. Bertulani; Phys. Rev. **C52**(1995)1706.

[17] B. Davids *et al.*, Phys. Rev. Lett. **81**(1998)2209.

[18] B. Davids *et al.*; Phys. Rev. Lett. **86**(2001)2750.

[19] T. Kikuchi *et al.*; Eur. Phys. J. **A3**(1998)213.

[20] F. Hammache *et al.*, Phys. Rev. Lett. **80**(1998)928, and nucl-ex/0101014.

[21] M. Hass et al., Phys. Lett. B462(1999)237.

[22] W.A. Fowler, Rev. Mod. Phys. **56**(1984)149.

[23] T.A. Weaver, and.E. Woosley; Physics Report, **227**(1993)65.

[24] M. Gai; In FROM THE SUN TO THE GREAT ATTRACTOR, Eds. D. Page and J.G. Hirsch, Lecture Notes in Physics, Springer, 2000, p. 49.

[25] A.G. Riess *et al.*; Astr. Jour. **116,3**(1998)1009.

[26] G.M. Hale; Nucl. Phys. bf A621(1997)177c.

[27] R. Kunz *et al.*; Phys. Rev. Lett. **86**(2001)3244.

[28] A Proposal: "A FREE-ELECTRON LASER GENERATED GAMMA-RAY BEAM FOR NUCLEAR PHYSICS", W. Tornow, R. Walter, H.R. Weller, V. Litvinenko, B. Mueller, P. Kibrough, Duke/TUNL, 1997.

[29] V.N. Litvinenko *et al.*, Phys. Rev. Letts. **78**(1997)4569.

[30] T. Shima, Y. Nagai, T. Kii, T. Baba, T. Takahashi, and H. Ohgaki; Nucl. Phys. **A629**(1998)475c.

[31] E.C. Schreiber *et al.*, Phys. Rev. **C61**(2000)061604(R).

[32] I. Tsentalovitch *et al.*; Bates proposal, 1999.

[33] U.Titt, A.Breskin, R.Chechik, V.Dangendorf, H.Schmidt-Bocking, H.Schuhmacher; A time projection chamber with optical read out for charged particle track structure imaging; Nucl. Instr. Meth. **A416**(1998)85. U.Titt, V.Dangendorf, H.Schuhmacher, Digital imaging of charged particle track structures with a low pressure optical Time Projection Chamber; Nucl. Phys. **B Supp. 78**(1999)444. U.Titt, Entwicklung einer optisch ausgelesenen Teilchenspurkammer fur dosimetrische und mikrodosimetrische Anwendungen. Dissertation zur Erlangung des Doktorgrades. (Ph.D. thesis), J.W.Goethe Universitat Frankfurt, 1999.

[34] Pausky *et al.*, Nucl. Instr. Meth. **354**(1995)262.